

Submitted Revised Manuscript

Selway, Nichola, Chan, Vincent and Stokes, Jason R. (2017). Influence of fluid viscosity and wetting on multiscale viscoelastic lubrication in soft tribological contacts. *Soft Matter* 13 (8) 1702-1715.

<https://doi.org/10.1039/c6sm02417c>

Influence of fluid viscosity on multi-scale viscoelastic friction in lubricated soft contacts

Nichola Selway, Jason R. Stokes*

*School of Chemical Engineering, The University of Queensland, Brisbane 4072, Queensland,
Australia.*

**Corresponding author:*

Professor Jason R. Stokes

*School of Chemical Engineering, The University of Queensland, Brisbane 4072, Queensland,
Australia.*

Tel: +61 (0) 7 3365 4361; Fax: +61 (0) 7 3365 4199

Email: jason.stokes@uq.edu.au

Nichola Selway

Email: nichola.selway@uqconnect.edu.au

Abstract

Friction (and lubrication) between soft contacts is prevalent in many natural and engineered systems and plays a crucial role in determining their functionality. The contribution of viscoelastic hysteresis losses to friction in these systems has been well-established and defined for dry contacts; however, the influence of fluid viscosity on these components of friction has largely been overlooked. We provide the first systematic experimental evidence of the influence of lubricant viscosity on lubrication across multiple regimes within a viscoelastic contact. This effect is investigated for comparatively smooth and rough contacts (PTFE ball on PDMS disc) lubricated by a series of Newtonian fluids, using a ball-on-disc tribometer. The distinct tribological behaviour, characterised generally by a decrease in the friction coefficient with increasing fluid viscosity, is explained in terms of multi-scale viscoelastic dissipation mechanisms at the bulk-, asperity- and molecular-scale. It is proposed that lubrication within the smooth contact is governed by molecular-scale (interfacial) viscoelastic effects, while fluid-asperity interactions within the rough contact stimulate additional rubber hysteresis at the asperity-scale, altering the general shape of the Stribeck curve. This fluid viscosity effect is in some agreement with theoretical predictions. Conventional methods for analysing and interpreting tribological data, which typically involve scaling sliding velocity with lubricant viscosity, need to be revised for viscoelastic contacts with consideration of these indirect viscosity effects.

Keywords (4-6 words): tribology; rubber; interfacial friction; roughness; viscoelastic hysteresis; viscoelastic dissipation

Abbreviations:

PDMS, polydimethylsiloxane; PTFE, polytetrafluoroethylene; SRR, slide-to-roll ratio;

1. Introduction

The study of soft-contact friction and lubrication is of great relevance to our fundamental understanding of biotribology and biological interface mechanics^{1,2}, but also has wide-reaching practical application in the design of bio-mimetics³, bio-inspired adhesives, biomedical devices e.g. prostheses⁴, rubber sealants⁵, and shaving devices. Tribological interactions at the tongue-palate and skin interfaces are also considered to play a key role in determining the functionality, including tactile perception, of food/beverages and personal care products (e.g. cosmetics, skin creams)⁶⁻⁹.

The tribological response of a lubricated system is determined by both hydrodynamics and surface contact forces. These two friction mechanisms are often considered in isolation (as discrete components) despite the complex interplay that exists between them. For example, under hydrodynamic (full-film) lubrication conditions, where the fluid pressure and lift force generated are sufficient to separate the opposing surfaces, the viscous drag of the lubricant is often considered to be the primary contributor to the friction force. However, fluid pressure acting on soft substrates can induce viscoelastic hysteresis losses that also contribute significantly to friction^{10,11}. Similarly, and perhaps more critically, the full extent of the role of lubricant viscosity in what is conventionally considered the ‘boundary’ and ‘mixed’ regimes has largely been overlooked in the case of compliant, viscoelastic contacts. We seek to address this oversight and emphasise its importance in the interpretation of tribological data.

It is widely accepted that the transition through different lubrication regimes occurs as a function of the ‘reduced velocity’, $U\eta$ (entrainment speed or sliding velocity multiplied by lubricant viscosity), which is also considered as the shear stress intensity acting across the contact zone, with units Pa.m or N/m. This characteristic parameter is a simplified version of the dimensionless Sommerfeld number $\left(\frac{\eta UR}{W}\right)$ or elastohydrodynamic number $\left(\frac{\eta UE^{1/3}R^{5/3}}{W^{4/3}}\right)$, for a particular tribo-system with defined (constant) sphere radius R , applied load W , and elastic modulus E . Thus it has become standard practice to interpret and present tribological data in the form of a Stribeck curve, with the friction coefficient as a function of $U\eta$. The term ‘Stribeck curve’ was originally developed for hard contacts to describe the frictional variation in the entire range of lubrication, including the hydrodynamic, mixed and boundary lubrication regimes. As this paper highlights, caution should be exercised when applying these conventional terms in soft-contact tribology, where lubrication regimes are less well-defined. However, for simplicity, the term ‘Stribeck curve’ is used here to refer to the overall friction profile for each lubricant.

The apparent collapse of tribological data for different viscosity fluids onto a single master curve by scaling with lubricant viscosity has been reported in many previous studies involving viscoelastic contacts. This master curve is often then used as a reference or baseline when comparing and interpreting the tribological behaviour of other more complex lubricants, such as multiphase fluids, or those containing adsorbent species¹². For such comparison, there is the assumption that any deviation from the master Stribeck curve can be attributed to non-hydrodynamic effects, such as adsorption and boundary layer formation¹³ and/or preferential entrainment or exclusion of particles in multiphase systems¹⁴⁻¹⁷. This has the potential to be a very powerful interpretive tool as it provides information about the fluid behaviour and composition localised in the contact zone. The same principle has also been used to estimate the average local shear rate and effective viscosity of non-Newtonian lubricants in the contact zone^{13, 18}. However, the underlying assumption that viscous effects are essentially ‘normalised’ through scaling with lubricant viscosity is not necessarily valid, leading to potential misinterpretation of tribological data. Therefore, it is necessary to develop new scaling laws for tribological analysis that incorporate the true effect of viscosity on friction and lubrication. We present experimental evidence and analysis on the influence of fluid viscosity and surface roughness on friction and lubrication in a viscoelastic contact. This work focusses on the mixed rolling and sliding tribological contact between a rigid sphere and a viscoelastic half space (i.e. ball-on-disc), lubricated by Newtonian fluids with varying viscosities.

There are two key reasons why the effect of viscosity has been overlooked in previous tribological studies involving viscoelastic contacts. Firstly, the friction coefficient is typically plotted on a log scale in order to observe the three lubrication regimes across a range of entrainment speeds. However, this renders it more difficult to visually distinguish between different viscosity lubricants (even when statistically significant differences may exist); hence an apparent collapse of data onto a single master curve is observed and reported. Secondly, the majority of experimental studies on lubrication within a viscoelastic contact use two opposing polydimethylsiloxane (PDMS) surfaces, owing to the material’s well-defined surface chemistry, elastomeric properties and biocompatibility. However, a PDMS-PDMS contact has a very high Coulombic (interfacial) friction. This component of the friction coefficient is dominant and the effect of lubricant viscosity on the overall Stribeck curve is less pronounced, though still evident for rough contacts, as noted by Bongaerts, Fourtouni et al.¹².

In this study, we utilise a tribo-system that exhibits a comparatively low Coulombic friction – polytetrafluoroethylene (PTFE) ball on PDMS disc – in order to clearly demonstrate the influence

of lubricant viscosity on rubber hysteresis effects in soft-tribology; that is, beyond its direct contribution to friction in the form of fluid viscous losses. An empirical model is fitted to the tribological data to obtain model parameters that describe the unique shape of each Stribeck curve. The model parameters are analysed as a function of lubricant viscosity and surface roughness, and the findings are discussed in terms of the four constituents of friction defined by Scaraggi and Persson's¹⁹ theory described below. This paper aims to validate aspects of their theoretical model, as well as highlight and address the potential for misinterpretation of experimental data due to a lack of integration with theoretical and numerical prediction.

2. Background

During rubbing (dry) contact, friction forces are considered to arise from the breaking of adhesive bonds formed at the contact interface^{20,21}, as well as subsurface deformation resulting from lateral motion and normal load^{22,23}. The latter constitutes an internal (cohesive) friction component relating to the viscoelastic dissipation of stressed molecules in the bulk material, commonly referred to as 'viscoelastic hysteresis losses' or 'deformation losses'^{24,25}. For highly compliant tribo-surfaces (e.g. elastomers), this internal cohesion is comparable to the interfacial adhesion and both dissipation processes have a significant contribution to the overall friction²⁶. Homogenised contact mechanics theories have recently enabled the effective calculation of hysteretic rubber friction for real (multi-scale) rough contacting surfaces²⁷. However, studies of friction involving viscoelastic solids have primarily focused on the contact mechanics of dry interacting surfaces, hence the influence of lubricant properties on hysteresis losses has only very recently been considered. Based on theoretical modelling of lubrication within viscoelastic contacts, Scaraggi and Persson¹⁹ extended the pioneering work of Hooke and Huang¹⁰ and Elsharkawy¹¹ to show that viscoelastic hysteresis generates an asymmetric fluid pressure field which can affect the Stribeck curve over a wide range of sliding speeds and lubrication regimes.

For lubricated soft contacts, four discrete components of friction need to be considered, as defined in Scaraggi and Persson's¹⁹ model:

- (i) solid-contact sliding friction, μ_{Sc}
- (ii) solid-contact rolling friction, μ_{Rc}
- (iii) wet-contact sliding friction, μ_{Sf}
- (iv) wet-contact rolling friction, μ_{Rf} .

The solid-contact sliding and rolling friction components represent the interfacial (adhesive) shear stress and rubber deformation losses, respectively, as mentioned earlier for dry contacts. Wet-contact sliding friction arises from shear stresses generated within the fluid contact regions and includes the contribution from both Poiseuille and Couette flow, while wet-contact rolling friction arises from a combination of fluid viscous losses and fluid-induced rubber deformation losses.

It is necessary to clarify a potential source of confusion here regarding the definition of rolling friction, which is considered to exist even for a pure sliding contact (200% slide-to-roll ratio, SRR). The term ‘rolling friction’ in this context simply represents the non-elastic effects that occur over the entire contact. For viscoelastic lubrication, this comprises rubber hysteresis losses as well as plastic deformation (fluid viscous losses). This is rationalised by considering that friction measured for a pure sliding contact that exhibits extremely low interfacial shear stress is (almost) equivalent to pure rolling friction ²⁸.

[Insert Figure 1]

Scaraggi and Persson ¹⁹ modelled each of these friction components as a function of reduced velocity, shown in Figure 1A and B for a low and high viscosity lubricant respectively. The summation of these four friction component curves yields the Stribeck curve (represented by the red line). The Stribeck curve is divided into distinct regions (denoted by the numbers 1 to 5), which are defined by both the rubber-to-glassy transition of the viscoelastic solid, and the prevalence of wet- versus solid-contact friction.

The rubbery region (1) occurs at low reduced velocities where the contact stress stored in the elastomer is capable of relaxing before an asperity can slip to the next contact site. The characteristic peak in solid-contact rolling friction defines the onset of the transition region (2) and is governed by the viscoelastic properties of the solid material. From dry elastomeric studies, this corresponds to the maximum in the loss modulus for smooth contacts and the maximum in the loss tangent for rough contacts ²⁵. Above the critical velocity, the material is unable to fully relax before the asperities are driven to the next contact site; hence the solid-contact rolling friction decreases as a result of fewer dissipative relaxation events ²⁶. The glassy region (3-5) occurs when the strain rate (governed by the sliding velocity) is too high for any molecular relaxation of the solid, meaning that there is no longer a contribution from the solid-contact rolling friction.

The classification of boundary (BL), mixed (ML) and hydrodynamic (HL) lubrication is dictated by the dominance of solid-contact friction (BL), the dominance of wet-contact friction (ML), or pure wet-contact friction (HL). As expected, the model predicts that solid-contact friction

dominates the Stribeck curve at low values of reduced velocity, whereas wet-contact friction has the greatest contribution at high reduced velocities where the conditions facilitate lubricant entrainment.

More interestingly, the model predicts that lubricant viscosity affects the relative contribution of solid-contact versus wet-contact friction across the range of reduced velocities, which can alter the shape of the Stribeck curve. This is evidenced by comparing Figures 1A and B, which demonstrates that the convention of scaling with lubricant viscosity is insufficient to achieve a master curve for lubrication in a viscoelastic contact. According to the model, an increase in lubricant viscosity stimulates additional rubber hysteresis due to fluid pressure acting on the asperities, leading to an increase in the wet-rolling friction (with respect to the wet-sliding friction). In rough contacts, these fluid-asperity interactions can occur at low reduced velocities, such that the wet-contact rolling curve coincides with the solid-contact rolling curve. The overlapping of these friction component curves (as observed in Figure 1B), alters the shape of the Stribeck curve, including a shift in peak friction to higher values of reduced velocity.

3. Materials and methods

3.1. *Tribo-surfaces*

Two different tribo-pairs were used in this study: (1) smooth PTFE ball-smooth PDMS disc, and (2) smooth PTFE ball-rough PDMS disc. The smooth PTFE balls were donated by Hoover Precision Products (Sault Ste Marie, Michigan, USA) and smooth PDMS balls were supplied by PCS instruments (London, United Kingdom). The PDMS discs were fabricated from a two-component silicone elastomer kit, Sylgard 184 (Dow Corning, Midland, Michigan, USA). The elastomer base and curing agent were combined in a ratio of 10:1 by mass and 3.2 mm thick sheets were cast in vertical aluminium-glass moulds. Smooth PDMS discs were produced by casting against the glass plate and rough discs were cast against a sandblasted aluminium plate. The PDMS sheets were cured in an 80°C oven for approximately 4 hours. After cooling, the PDMS sheets were removed from the moulds and discs ($D = 48$ mm) were cut from the sheets. The r.m.s. surface roughness of the surfaces were characterised using a stylus profilometer (Dektak 150, Veeco, New York) and are presented in **Error! Reference source not found.**

[Insert Table 1]

3.2. *Lubricant systems*

The lubricants used in this study are glycerol-water mixtures, ranging from 0 to 60% glycerol (ChemSupply). The densities and viscosities of these Newtonian fluids at 35°C are given in Table 2. Viscosities were determined using size 50 and 100 series Canon-Fenske glass capillary viscometers (Cannon Instrument Company, State College, Pennsylvania, USA) in a temperature-controlled water bath.

[Insert Table 2]

3.3. *Tribological measurement*

The tribological properties of the glycerol-water systems were characterised using a ball-on-disc tribometer (MTM2, PCS Instruments Ltd, London, United Kingdom) fitted with compliant contacts. The friction force F_f was measured as a function of the entrainment speed, U , defined as the average surface speed of the ball and disc, $U = (U_{ball} + U_{disc})/2$, over the range of 1 to 3000

mm/s in logarithmic intervals. Measurements were carried out for six repetitions of alternately descending and ascending entrainment speed. For all tests, a normal load (W) of 2 N was applied on the ball and a SRR of 50% was used to impart both sliding and rolling motion, where $SRR = |U_{ball} - U_{disc}|/U$. The friction coefficient (μ) is calculated as the friction force divided by applied load ($\mu = F_f/W$). According to Hertzian contact mechanics, the PTFE-PDMS tribo-contact under the load tested would have an indentation depth of approximately 180 μm and an apparent contact radius of 1.30 mm (calculations provided in Supplementary Information).

The lubricants were maintained at the desired test temperature of 35°C (to reflect a typical biological system) using a silicone oil temperature bath (DC30-K20, Haake) and samples were pre-heated in a circulatory water bath. Prior to testing, the PDMS contacts were cleaned by gently rubbing the surface with a lens-cleaning wipe soaked in 1% SDS solution. They were then ultrasonicated in 1% SDS solution, followed by thorough rinsing and ultra-sonication in RO water to remove all surfactant molecules.

At low entrainment speeds, the load and SRR can become unstable as a result of stick-slip behaviour arising from relatively strong adhesion between tribo-surfaces. Hence, all tribological data is filtered to eliminate data points that do not satisfy the following tolerances: $45\% < SRR < 55\%$ and $1.9 < W < 2.1\text{N}$. Due to the self-adhesive nature of PDMS, low speed instabilities resulted in considerable loss of data for the PDMS-PDMS tribopairs; hence, this paper focusses on the data obtained for the PTFE-PDMS tribopairs only. The Stribeck curve for each lubricant is fitted with an empirical model, as defined by Bongaerts, Fourtouni et al. ¹²:

$$\mu_{total} = \mu_{EHL} + \left(\frac{\mu_b - \mu_{EHL}}{1 + \left(\frac{U\eta}{B}\right)^m} \right)$$

where $\mu_{EHL} = k(U\eta)^n$ and $\mu_b = h(U\eta)^l$.

3.4. Contact Angle Measurement

The contact angles of all glycerol-water systems were characterised in air on rough and smooth PDMS substrates using an OCA20 contact angle goniometer (Data Physics Corporation, San Jose, California, USA). Still images of 10 μL droplets were taken after a contact time of 10 seconds and analysed according to the Pendant drop method, using the SCA20 software. Both left and right contact angles were determined and averaged since no significant difference was observed. The

contact angles of eight droplets were determined for each lubricant-substrate combination and the average values are presented in Table 3. All contact angle measurements were performed at ambient temperature (approximately 23°C) since no temperature control was available. The discrepancy in temperature between the tribological and contact angle measurements is considered to have minimal impact since contact angle only has a weak dependence on temperature²⁹.

[Insert Table 3]

4. Results and discussion

4.1. General shape of the Stribeck curve

The lubrication profiles of a series of glycerol-water mixtures with a range of dynamic viscosities are characterised within a viscoelastic contact to investigate lubricant viscosity effects. Figure 2 shows the friction coefficient as a function of entrainment velocity for a PTFE ball in tribological contact with (A) a smooth and (B) a rough PDMS disc. The same general trend in tribological data is observed for both tribo-pairs and across the range of lubricant systems – the friction coefficient increases logarithmically with entrainment velocity up to a critical velocity, beyond which it decreases. At very high entrainment velocities, a minimum in the friction coefficient is observed for the highest viscosity fluids in the smooth contact (visible on a log-log plot). This characteristic shape is predicted by Scaraggi and Persson's¹⁹ theoretical model and can be explained in terms of the dissipation mechanisms at play in the tribological contact. Figure 3A and B show the same friction coefficient data as in Figure 2, plotted as a function of the reduced velocity, i.e. the entrainment speed multiplied by lubricant viscosity, $U\eta$. The rubber-to-glassy transition regions of the Stribeck curve, as defined in their model, are more clearly observed in this format (as labelled). The tribological profiles are fitted with an empirical equation proposed by Bongaerts, Fourtouni et al.¹² and the corresponding model parameters, which characterise the unique shape of each curve, are discussed in Section 4.3 in terms of viscosity and roughness effects.

[Insert Figure 2 and 3]

Below the critical velocity, the friction force for all lubricants is shown to increase logarithmically with velocity, which is consistent with an activated molecular relaxation process occurring in the PDMS³⁰ i.e. the viscoelastic substrate is in a rubbery state. Based on Scaraggi and Persson's¹⁹ theoretical model, the characteristic peak in friction coefficient observed for all lubricant systems is governed by the solid-contact rolling friction and represents the competition between the characteristic time-scale of the tribological process (i.e. the loading and unloading time) versus the relaxation time of the PDMS. For dry contacts, the maximum dissipation (and rolling friction) occurs when the time of loading/unloading coincides with the relaxation time of the material²⁶. Beyond this critical velocity, the internal relaxation of the PDMS is slower than the loading/unloading time, leading to a decrease in viscoelastic dissipation (solid-contact rolling friction) and marking the onset of the transition region. This time-scale imbalance is also predicted to lead to an increase in the effective elastic modulus of the PDMS with increasing velocity, and subsequently, a reduction in contact area and solid-contact sliding friction. It should be noted that,

for the lubricated contacts studied here, the critical velocity corresponding to the peak in friction could also be affected by fluid-asperity interactions (wet-rolling friction), especially at higher lubricant viscosities. This is discussed in more detail later. At even higher reduced velocities, the tribological time-scale is much faster than the relaxation time and the deformation of PDMS is primarily elastic i.e. in a glassy state. The glassy region is observed here only for the smooth contact, as labelled in Figure 3A.

An important point should be emphasised here with regards to defining and labelling lubrication regimes. The decrease in friction coefficient beyond the critical velocity, observed here for all lubricants, is commonly considered to indicate the onset of the mixed lubrication regime; that is, the transition from an asperity-dominated contact to one that is dominated by fluid hydrodynamics. However, the model of Scaraggi and Persson¹⁹ highlights that the ‘true’ transition point between the boundary, mixed and hydrodynamic regimes for viscoelastic contacts does not necessarily coincide with the minima and maxima in the Stribeck curve. This decrease in friction can equally occur due to a ‘stiffening’ of the contact due to the competing time-scales described above. This interpretation is contrary to many experimental studies in the field, since they were developed from more traditional tribological studies involving harder substrates. The inability to easily define the transitions in viscoelastic contacts suggests that theoretical and numerical modelling play a crucial role in developing an enhanced mechanistic understanding of the underlying dissipation processes, which can then be applied to more accurately interpret experimental data, as exemplified in this paper.

Friction data for the dry contacts are also included in Figure 2. For the smooth contact (Figure 2A), the friction coefficient monotonically increases with entrainment speed for the range tested, whereas an apparent plateau or maximum is observed for the rough contact (Figure 2B). It is anticipated that for higher velocities (beyond the current measurement limitations), a decrease in friction coefficient would also be observed for the dry contacts; this is supported by dry elastomeric friction studies that show a destabilisation beyond a critical velocity when stick-slip sliding occurs and the contact area shrinks from adhesive (JKR) to Hertzian³¹.

4.2. Influence of lubricant viscosity

It is immediately clear in Figure 3A and B that, for both smooth and rough tribopairs, there is no collapse of the data onto a single Stribeck master curve, as may typically be anticipated after

scaling. Instead, the friction coefficient decreases with increasing viscosity over a wide range of $U\eta$ values. It is also observed that the Stribeck curves generated for the smooth contact maintain a similar shape as a function of viscosity, whereas a loss of vertical symmetry in the friction curve is seen for the rough contact. This roughness effect is discussed in detail in Section 4.3. The differentiation between the tribological profiles of various Newtonian lubricants indicates that fluid viscosity has an impact on lubrication beyond its direct contribution to wet-contact sliding friction (Couette and Poiseuille friction). Hence, it is necessary to consider the effect of viscosity on the remaining three identified components of friction: solid-contact rolling, wet-contact rolling, and solid-contact sliding friction.

We propose a multi-scale viscoelastic conceptual model, illustrated in Figure 4, to explain the observed lubrication behaviour and the role of fluid viscosity and surface roughness. This explanation is based on the coexistence of multiple viscoelastic dissipation mechanisms (labelled I, II and III), which have traditionally been considered independently in the literature. However, it is proposed that the overall friction profiles of the lubricated system studies here are determined by the complex interplay and competition between these three processes.

On the macroscale (I), viscoelastic hysteresis is induced by bulk deformation of the PDMS disc, i.e. solid-contact rolling friction. Lubricant viscosity is not anticipated to have a direct effect on this component of viscoelastic dissipation since it relates to internal (subsurface) cohesion of the PDMS elastomer.

At the asperity scale (II), however, fluid pressure generated between asperities induces viscoelastic hysteresis in the PDMS, and the associated relaxation time of the rubber asperities is dependent on the lubricant viscosity. This is rationalised by considering the asperities as discrete entities, whose relaxation behaviour reflects single-molecule hydrodynamic theory, which predicts that the time for reorientation of a molecule is proportional to the solvent viscosity divided by the temperature^{32,33}. Hence, the wet-contact rolling friction profile is anticipated to be a function of fluid viscosity, arising from this competition between asperity relaxation rate and the strain rate of the tribological process. Therefore, rolling friction for wet contacts cannot be estimated using theory and experimental data from dry contact studies due to the contribution of these fluid-asperity interactions¹⁹. These fluid-asperity interactions are, of course, more pronounced for rough contacts, as demonstrated in Section 4.3.

At a molecular level (III), interfacial shear stress (solid-contact sliding friction) arises from the formation of adhesive bonds between the two solid substrates. These adhesive bonds are formed from polymer linkages, which become stretched under shear until they debond, relax and reattach, as shown in the schematic diagram. This mechanism is described in literature for dry elastomeric

friction³¹. The viscosity of the confined fluid film (if present) is anticipated to govern this molecular motion, including bonding and relaxation times, thereby influencing the interfacial shear stress. Stronger interfacial interactions also result in additional bulk deformation and thus solid-contact rolling friction could be indirectly influenced by lubricant viscosity.

[Insert Figure 4]

In consideration of these multi-scale viscoelastic effects, the decrease in friction coefficient with increasing viscosity observed here for both tribo-pairs is attributed to the effect of lubricant viscosity on the adhesion (interfacial) viscoelastic dissipation of the interfacial elastomer molecules in bonding and debonding events. Once again, hydrodynamic theory for single-molecules predicts that an increase in lubricant viscosity corresponds to a slower relaxation time of the interfacial PDMS molecules and deeper potential energy wells exist which restrict molecular motion and less adhesive bonds are able to form. In other words, for a given sliding velocity (or loading/contact time), the molecules are less effective in facilitating interfacial adhesion; hence, interfacial shear stress and friction decrease. The reduction in the maximum friction coefficient with increasing viscosity represents a notable deviation from Scaraggi and Persson's theoretical model. This is considered to arise from their assumption that the solid-contact shear stress is independent of the lubricant viscosity. However, the findings presented here suggest that lubricant viscosity does influence the molecular dynamics at the rubbing interface and hence affects the interfacial friction.

A recurring challenge associated with experimental studies into the effect of fluid viscosity on system properties such as lubrication is that the viscosifying agent can have other physicochemical effects on the system, which render it difficult to irrefutably determine causality. It is important here to consider the possibility that glycerol molecules present in the tribological system could associate with the interacting surfaces to generate an effect on the lubrication profile that is unrelated to viscosity. However, the contact angle measurements of glycerol-water solutions on PDMS (in air) are shown to be independent of glycerol concentration for both smooth and rough substrates (see Table 3), which suggests that glycerol does not undergo surface adsorption to form a boundary layer. Hence, it is considered that the distinct tribological profiles generated by different glycerol-water lubricants are primarily due to viscosity effects. However, the potential for such competing effects again highlights the value of mechanistic modelling in conjunction with experimental studies to isolate the role of fluid viscosity.

4.3. Viscoelastic lubrication in smooth versus rough contacts

There are several key differences in the tribological profiles generated using the smooth versus rough PDMS disc, which provide some insight into the dissipation mechanisms that govern the friction produced in each case.

Firstly, the peak friction values are lower in the case of the rough surface for all viscosities tested, although there is less discrepancy at high viscosities, as shown in Figure 5A. This reduction in friction with increasing roughness is considered to be the net result of three competing effects. Firstly, the solid-contact sliding friction is expected to decrease with increasing surface roughness due to a reduction in the real area of contact available for interfacial interaction between the two solid surfaces. A further decrease in the solid-contact rolling friction arises from the increase in the apparent contact area (due to surface irregularities) which results in a reduction in nominal contact pressure and indentation depth. However, this reduction in bulk deformation is counteracted by additional contributions to the solid-contact rolling friction from asperity deformation. In contrast, stronger interfacial interactions in the case of the smooth contact are anticipated to drive additional bulk deformation and contribute to the higher measured friction, compared to the rough contact. Note that friction generated by the interlocking of opposing asperities is expected to be minimal in this case, since the ball roughness is much smaller than the disc roughness. However, a comparison between a ‘rough ball on rough disc’ and ‘smooth ball on smooth disc’ may yield considerably different results due to the potential for ‘interlocking friction’ between two rough surfaces.

It is also observed that the maximum in the friction coefficient occurs at a higher velocity for the rough compared to the smooth surface – a trend reported previously for dry viscoelastic contacts³⁴. However, this trend is also supported by Scaraggi and Persson’s model for wet contacts, which predicts that the critical velocity corresponding to the maximum in the solid-contact rolling friction (v_{GT}) occurs when $v_{GT} \approx a_0/\tau_r$ (i.e. the Hertzian contact radius divided by the rubber relaxation time). Since the width of the apparent contact area increases with surface roughness, the critical velocity is also expected to increase with roughness. More interestingly, however, are the differences in the friction profiles as a function of viscosity.

The rate of decrease in peak friction with increasing viscosity is higher for the rough surface, as shown in Figure 5A. It is also evident that, in the smooth case, the same general shape in the Stribeck curve is maintained as a function of viscosity, whereas for the rough contact, the friction peak flattens with increasing viscosity and there is a loss of symmetry in the data as compared to the smooth surface. Some of these differences may be subtle in a visual context, however, upon extraction of the empirical equation parameters from data fitting, we are able to observe clear

systematic changes in the curve. Again, the multi-scale viscoelastic dissipation mechanisms illustrated in Figure 4 can be used to explain the differences between smooth and rough contacts with regards to their lubrication behaviour as a function of fluid viscosity.

[Insert Figure 5]

As shown in Figure 5B, the slope of the rubbery region decreases with increasing viscosity for rough surfaces, whereas it is relatively constant for smooth surfaces. This could be explained by the fact that, at the lowest values of reduced velocity, the friction coefficient is dominated by shear adhesion, and shear forces associated with deformation of the asperities. Therefore, in rough contacts, an increase in speed generates a localised hydrodynamic lift force, which increases the film thickness, leading to less contact area for adhesion and less solid to deform. Friction coefficient still increases with speed due to the increase in solid-contact rolling friction, but to a lesser extent.

Figure 5C shows the reduced velocity at the peak in friction, $(U\eta)_T$, as a function of lubricant viscosity for both smooth and rough contacts. For the smooth case, the transition velocity remains constant with lubricant viscosity; however, for the rough contact there is a shift in the peak friction to higher $U\eta$ values with increasing fluid viscosity. This is also illustrated in Figure 3B, where the dotted line shows the onset of the transition region, which increases with lubricant viscosity. This trend is in alignment with the model predictions¹⁹ reported by Scaraggi and Persson for a rough, viscoelastic contact. The dotted line in Figure 5C shows the critical reduced velocities predicted by Scaraggi and Persson's model, which are also shown to increase with lubricant viscosity, but are notably lower than the experimental values here. However, the slope at relatively high viscosity is comparable between the theoretical and experimental data for the rough contact, suggesting the data follow a similar mechanism but are shifted in absolute magnitude. The discrepancy between the model predictions and experimental data presented here can be attributed to model assumptions regarding substrate properties (e.g. multiscale roughness, viscoelastic properties).

The shift in peak friction to higher $U\eta$ values as viscosity increases for rough, but not smooth, surfaces can be explained in terms of the asperity-scale viscoelastic effects described in Section 4.2. The transfer of normal load from the asperity contacts to the fluid pooled between asperities increases the locally averaged fluid pressure, which results in the PDMS substrate being hysteretically stimulated by the fluid-asperity interactions i.e. wet-rolling friction. Both the wet-contact rolling and wet-contact sliding friction are present at much lower reduced velocities in the rough compared to the smooth contact due to the availability of fluid between the asperities. This affects the shape of the resulting Stribeck curve. As the viscosity increases, the viscoelastic relaxation of the asperities slows down and the maximum wet-rolling friction occurs at higher

reduced velocities, leading to a flattening of the friction peak and a shift to higher reduced velocities.

These results suggest that, for rough surfaces, the influence of fluid viscosity is governed by both asperity-scale viscoelastic dissipation and molecular-scale interfacial dissipation, whereas for smooth surfaces, the influence of fluid viscosity is dominated by molecular-scale effects. These findings reflect previous research on dry contacts which suggests that molecular (interfacial) interactions dictate friction in smooth contacts, since the ratio of the velocity corresponding to the peak in friction coefficient and the frequency corresponding to the peak in loss modulus, yields a constant length equivalent to the molecular dimension of the viscoelastic solid used³⁵. Similarly, for rough contacts, the velocity corresponding to the peak in friction coefficient and the frequency corresponding to the maximum in loss tangent, yields a constant length consistent with the average spacing between asperities. This is considered to indicate that friction on rough surfaces arises from the viscoelastic dissipation of the deformed asperities³⁴⁻³⁶.

5. Conclusions

Lubricant viscosity is shown to have a considerable effect on the tribological profiles of glycerol-water systems in smooth and rough viscoelastic contacts over a wide range of reduced velocity values. In both cases, the friction coefficient decreases with increasing lubricant viscosity, attributed to fluid-substrate interactions and their impact on viscoelastic energy dissipation at multiple length scales. It is proposed that the influence of fluid viscosity on lubrication within the smooth contact is governed by molecular-scale (interfacial) viscoelastic effects, whereby more viscous fluids reduce friction by slowing down the molecular bonding/debonding events responsible for adhesion. Interfacial effects are less dominant in the rough contact due to the reduction in real contact area; however, an additional component of friction arises from fluid-asperity interactions within the rough contact, which stimulate additional rubber hysteresis at the asperity-scale, altering the general shape of the Stribeck curve. Conventional scaling with lubricant viscosity is shown to be insufficient to achieve a master curve and indirect viscosity effects on lubrication need to be considered when interpreting tribological data. These findings give rise to numerous avenues for future research (experimental, theoretical and numerical) focussed on the influence of fluid-substrate interplay on friction mechanisms within soft contacts, particularly for lubricant systems that exhibit greater rheological complexity (e.g. viscoelastic fluids, particle suspensions). The insight generated from such studies have the potential to be applied in the

engineering of novel materials, systems and products with targeted functionality, as well as providing an enhanced understanding of natural lubrication processes.

Acknowledgements

The authors would like to acknowledge funding from The University of Queensland (UQ Advantage Scholarship) and the Australian Postgraduate Award (APA Scholarship), as well as support via the Australian Research Council Linkage Grant (ARC LP140100952) and PepsiCo (USA). Vincent Chan is also acknowledged for performing contact angle measurements. Gratitude is also extended to colleagues from the Rheology, Tribology and Biointerfaces research group at UQ for insightful discussions, especially Dr. Gleb Yakubov and Grace Dolan.

References

1. M. J. Adams, B. J. Briscoe and S. A. Johnson, *Tribology Letters*, 2007, **26**, 239-253.
2. A. Dunn, J. Urueña, Y. Huo, S. Perry, T. Angelini and W. G. Sawyer, *Tribology Letters*, 2013, **49**, 371-378.
3. A. E. Kovalev, M. Varenberg and S. N. Gorb, *Soft Matter*, 2012, **8**, 7560-7566.
4. G. A. Ateshian, *Journal of Biomechanics*, 2009, **42**, 1163-1176.
5. M. Scaraggi and G. Carbone, *Advances in Tribology*, 2012, **2012**, 12.
6. J. Chen and J. R. Stokes, *Trends in Food Science and Technology*, 2011, **25**, 4-12.
7. R. A. de Wijk and J. F. Prinz, *Food Quality and Preference*, 2005, **16**, 121-129.
8. M. E. Malone, I. A. M. Appelqvist and I. T. Norton, *Food Hydrocolloids*, 2003, **17**, 763-773.
9. N. Selway and J. R. Stokes, *Annual Review of Food Science and Technology*, 2014, **5**, 373-393.
10. C. J. Hooke and P. Huang, *Proceedings of the Institution of Mechanical Engineers, Part J: Journal of Engineering Tribology*, 1997, **211**, 185-194.
11. A. A. Elsharkawy, *Wear*, 1996, **199**, 45-53.
12. J. H. H. Bongaerts, K. Fourtouni and J. R. Stokes, *Tribology International*, 2007, **40**, 1531-1542.
13. J. R. Stokes, L. Macakova, A. Chojnicka-Paszun, C. G. De Kruif and H. H. J. De Jongh, *Langmuir*, 2011, **27**, 3474-3484.
14. D. A. Garrec and I. T. Norton, *Food Hydrocolloids*, 2013.
15. J. de Vicente, H. A. Spikes and J. R. Stokes, *Journal of Tribology*, 2006, **128**, 795-800.
16. D. M. Dresselhuis, H. Klok, M. A. C. Stuart, R. de Vries, G. A. van Aken and E. H. A. de Hoog, *Food Biophysics*, 2007, **2**, 158-171.
17. G. A. van Aken, M. H. Vingerhoeds and R. A. de Wijk, *Food Hydrocolloids*, 2011, **25**, 789-796.
18. J. de Vicente, J. R. Stokes and H. A. Spikes, *Tribology International*, 2005, **38**, 515-526.
19. M. Scaraggi and B. N. J. Persson, *Tribology International*, 2014, **72**, 118-130.
20. Y. B. Chernyak and A. I. Leonov, *Wear*, 1986, **108**, 105-138.

21. A. Schallamach, *Wear*, 1963, **6**, 375-382.
22. F. P. Bowden and D. Tabor, *Journal*, 1964.
23. A. M. Bueche and D. G. Flom, *Wear*, 1959, **2**, 168-182.
24. K. C. Ludema and D. Tabor, *Wear*, 1966, **9**, 329-348.
25. K. A. Grosch, *Proceedings of the Royal Society of London A: Mathematical, Physical and Engineering Sciences*, 1963, **274**, 21-39.
26. S. Sills, K. Vorvolakos, M. Chaudhury and R. Overney, in *Fundamentals of Friction and Wear*, eds. E. Gnecco and E. Meyer, Springer Berlin Heidelberg, 2007, DOI: 10.1007/978-3-540-36807-6_30, ch. 30, pp. 659-676.
27. B. N. J. Persson, *The Journal of Chemical Physics*, 2001, **115**, 3840-3861.
28. J. A. Greenwood and D. Tabor, *Proceedings of the Physical Society*, 1958, **71**, 989.
29. J. C. Berg, *An introduction to interfaces & colloids : the bridge to nanoscience*, World Scientific, New Jersey, 2010.
30. S. Sills, K. Vorvolakos, M. K. Chaudhury and R. M. Overney, in *Fundamentals of Friction and Wear*, eds. E. Gnecco and E. Meyer, Springer Berlin Heidelberg, Berlin, Heidelberg, 2007, DOI: 10.1007/978-3-540-36807-6_30, pp. 659-676.
31. K. Vorvolakos and M. K. Chaudhury, *Langmuir*, 2003, **19**, 6778-6787.
32. A. Einstein, *Annalen der Physik*, 1906, **19**, 371-381
33. P. Debye, *Journal*, 1929.
34. X.-D. Pan, in *Polymer Adhesion, Friction, and Lubrication*, John Wiley & Sons, Inc., 2013, DOI: 10.1002/9781118505175.ch11, pp. 443-499.
35. K. A. Grosch, *Rubber Chemistry and Technology*, 2007, **80**, 379-411.
36. M. K. Chaudhury, K. Vorvolakos and D. Malotky, in *Polymer Thin Films*, eds. O. K. C. Tsui and T. P. Russell, World Scientific, Singapore, 2008, pp. 195–219.

Table 1 - Surface roughness of tribo-surfaces, measured using a stylus profilometer.

Tribo-surface	Surface roughness (r.m.s) (μm)
Smooth PTFE ball	0.41 ± 0.08
Smooth PDMS disc	0.39 ± 0.07
Rough PDMS disc	5.2 ± 0.6

Table 2 - Densities and viscosities for glycerol-water lubricant systems.

Glycerol Conc. (wt%)	Density at 35°C (g/mL)	Dynamic Viscosity at 35°C (mPas)
0	0.99	0.73
10	1.02	0.91
20	1.05	1.20
30	1.08	1.64
40	1.10	2.30
45	1.11	2.89
50	1.12	3.57
55	1.14	4.68
60	1.15	6.01

Table 3 - Contact angles of glycerol-water mixtures on PDMS in air.

Glycerol Conc. (wt%)	Contact angle on PDMS ($^{\circ}$)	
	Smooth	Rough
0	97.4 ± 0.9	116 ± 1.1
10	98.9 ± 2.5	115 ± 1.6
20	96.3 ± 0.9	106 ± 0.9
30	96.2 ± 0.9	110 ± 2.2
40	96.2 ± 0.5	111 ± 1.1
50	96.6 ± 1.1	108 ± 1.2
60	95.9 ± 0.6	105 ± 1.3

Figure captions:

Figure 1. Scaraggi and Persson's theoretical model for viscoelastic lubrication for a (A) low and (B) high viscosity lubricant, showing the four key components of friction and their summation which yields the Stribeck curve (red). Several distinct regions of the Stribeck curve (numbered 1 to 5) can be identified by superimposing these component curves. Reproduced from Scaraggi and Persson¹⁹.

Figure 2. The friction coefficient as a function of entrainment velocity for the series of glycerol-water mixtures, as well as the dry contact, for a PTFE ball in tribological contact with (A) a smooth and (B) a rough PDMS disc. The friction curves for all lubricants exhibit a characteristic shape, which is predicted by theoretical models and explained in terms of viscoelastic dissipation mechanisms.

Figure 3. The same friction data as in Figure 2, for the series of glycerol-water mixtures, plotted as a function of reduced velocity, $U\eta$ (entrainment speed multiplied by lubricant viscosity) for (A) a smooth and (B) a rough PTFE-PDMS contact. Different regions of the Stribeck curve, defined by the transition from a rubbery to glassy response of the viscoelastic PDMS, are observed and indicated by the dotted lines.

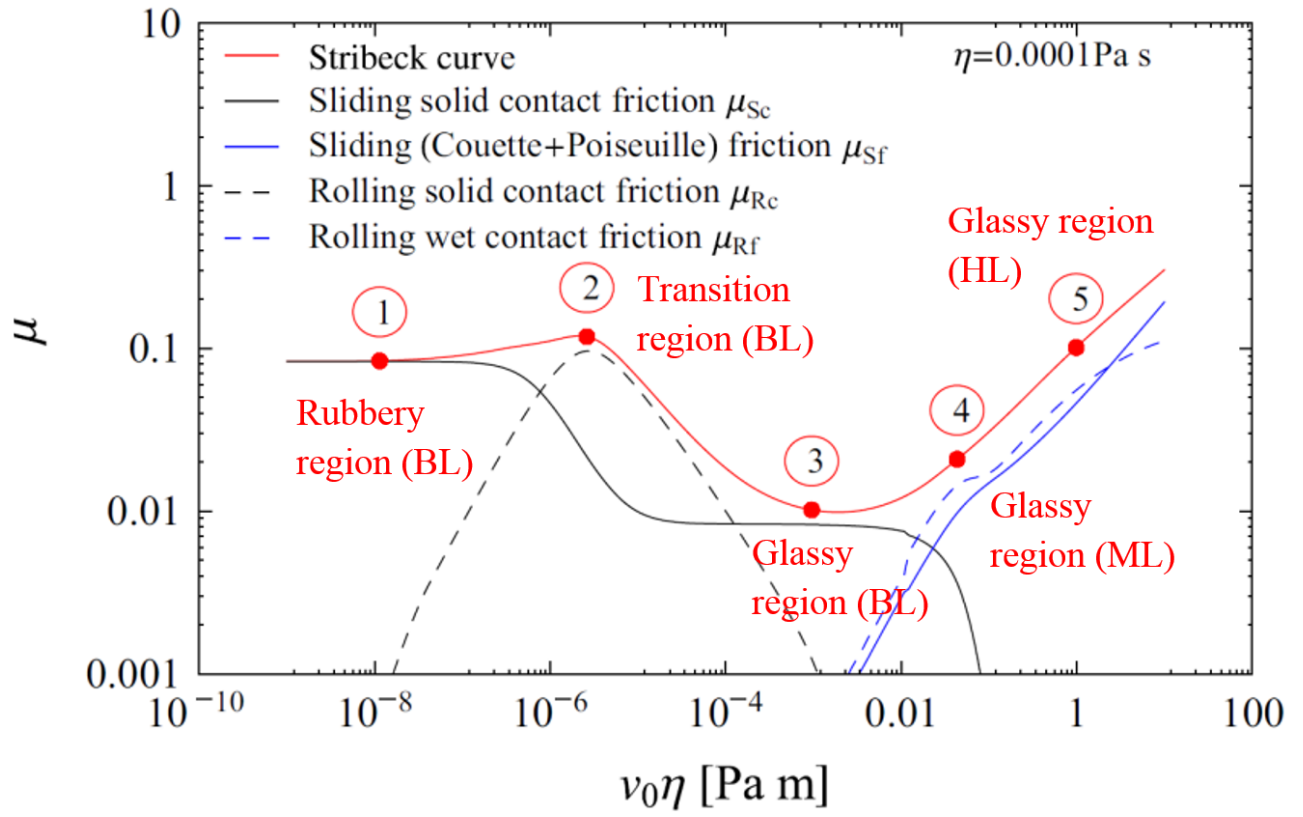
Figure 4. The multi-scale viscoelastic conceptual model proposed to explain the influence of lubricant viscosity on the tribological profiles of a smooth and rough contact. The schematic illustrates three key viscoelastic dissipation mechanisms operating at the macro- (bulk), asperity- and molecular-scale.

- (I) Macro-scale: bulk deformation of the rubber (PDMS) induces viscoelastic hysteresis (solid-contact rolling friction), which peaks in value when the rubber relaxation time coincides with the tribological (un)loading time.
- (II) Asperity-scale: fluid pressure generated between asperities induces viscoelastic hysteresis in the PDMS, and the resulting wet-contact rolling friction is dependent on the lubricant viscosity.
- (III) Molecular-scale: interfacial shear stress (solid-contact sliding friction) arises from adhesive bonds in the form of polymer linkages between the two surfaces, which become stretched under shear until they debond, relax and reattach. The kinetics of this molecular motion is considered to be affected by the viscosity of the confined fluid film.

Figure 5. Model parameters that define distinguishing features the Stribeck curves, plotted as a function of lubricant viscosity: (A) peak friction; (B) logarithmic slope of the rubber region; (C) critical reduced velocity, corresponding to the peak in the friction curve. Key differences in the tribological profiles generated using the smooth versus rough PDMS disc are highlighted, and provide insights into the governing dissipation mechanisms and the related role of viscosity.

Figure 1

A



B

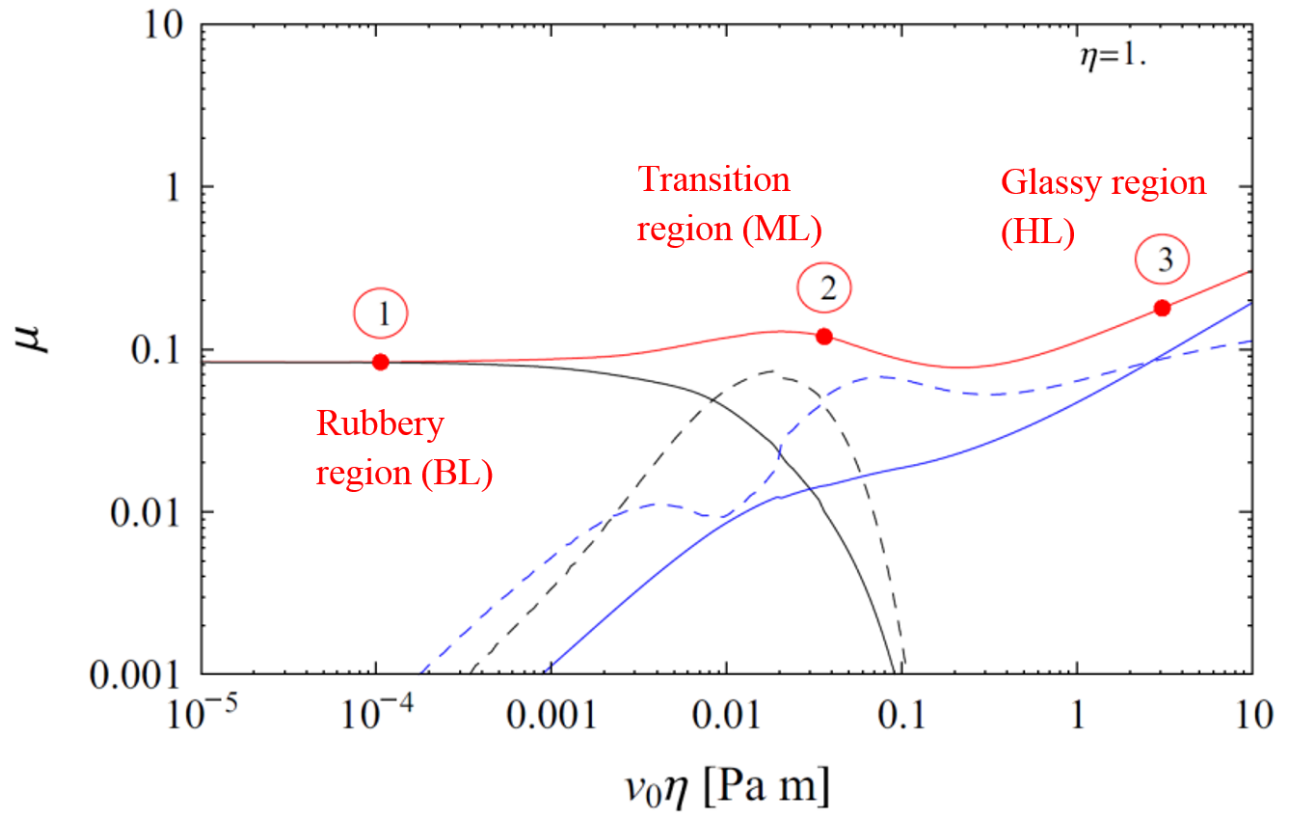


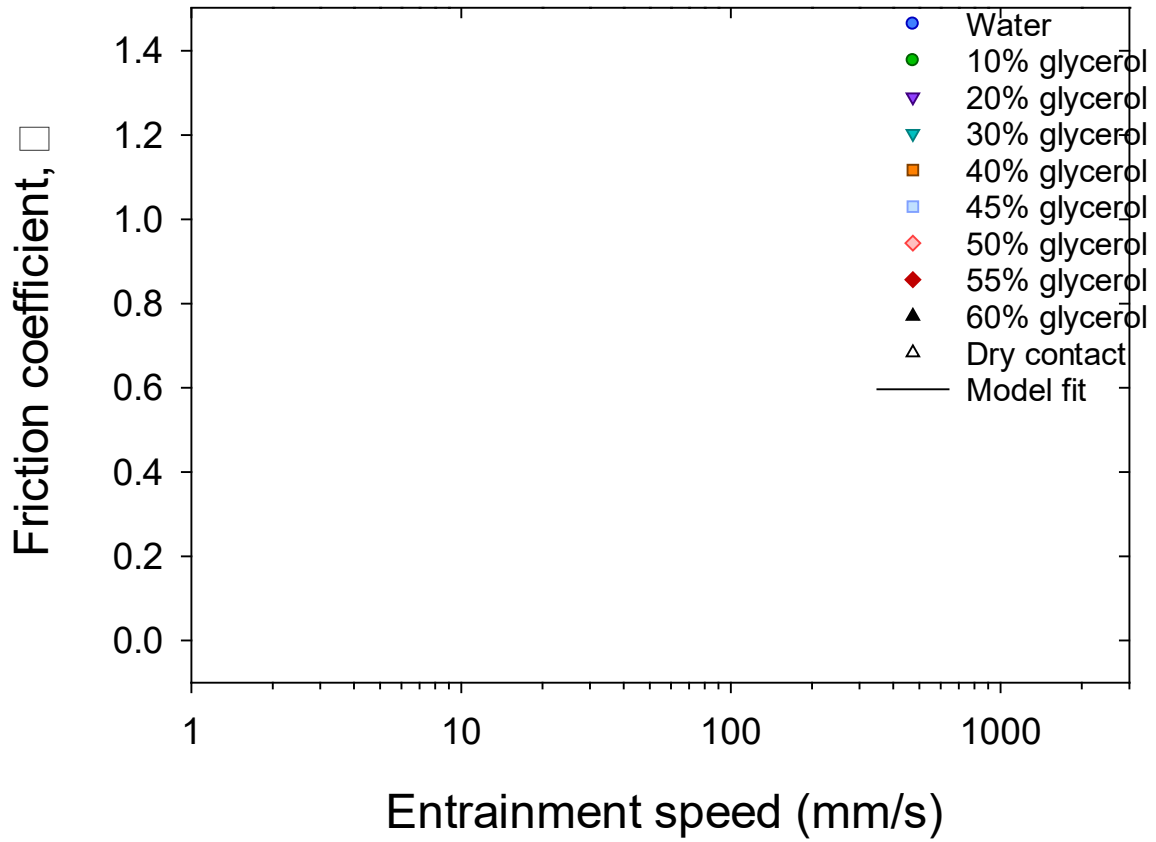
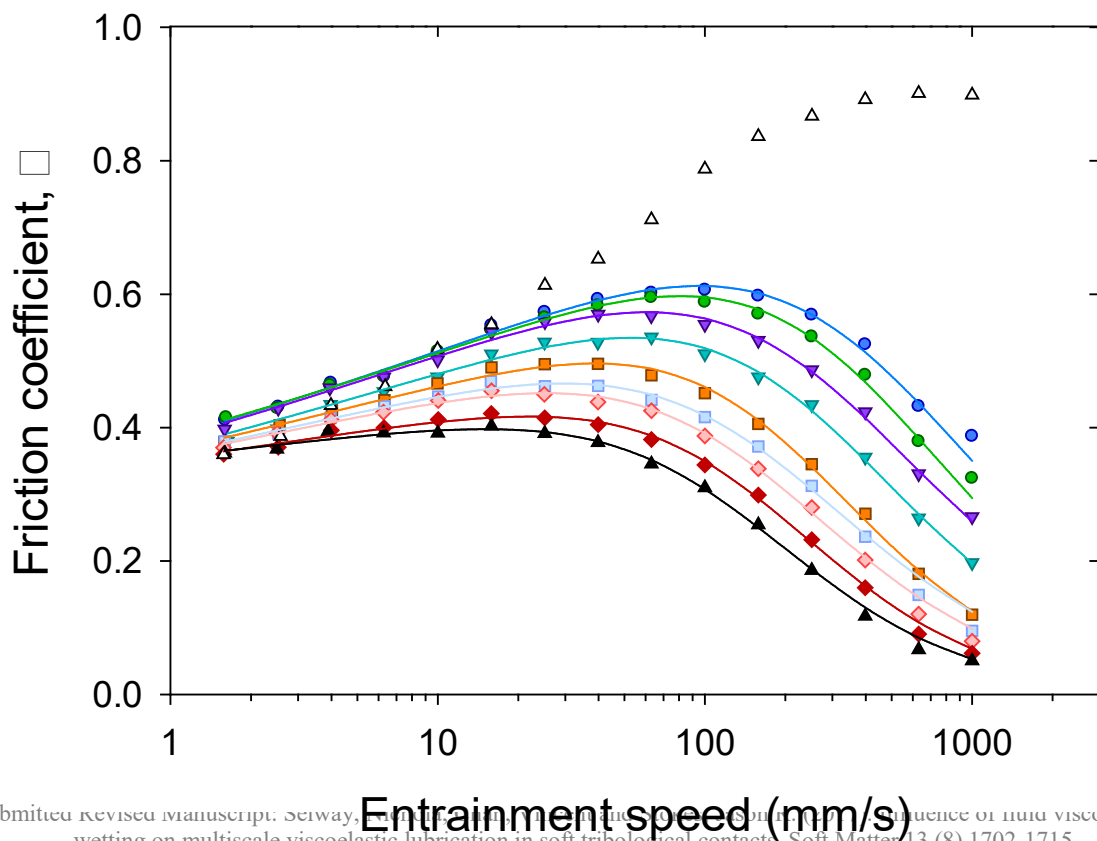
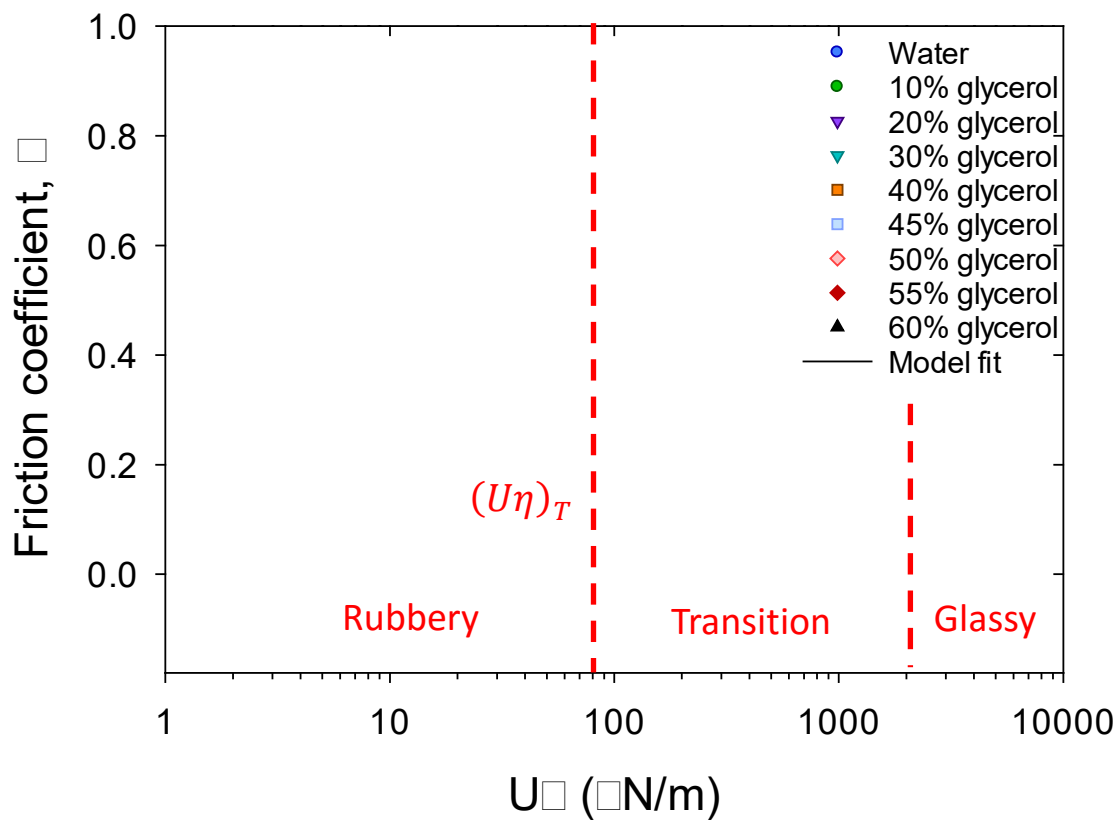
Figure 2**A****B**

Figure 3

A



B

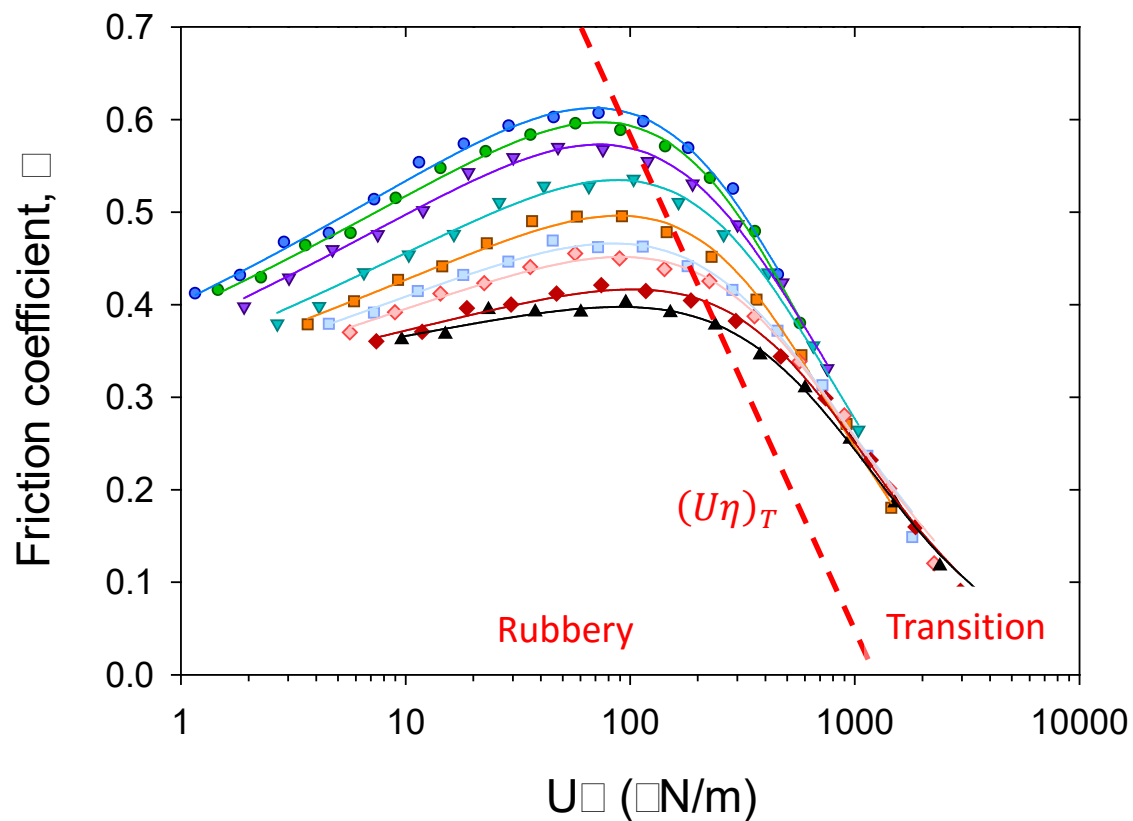


Figure 4

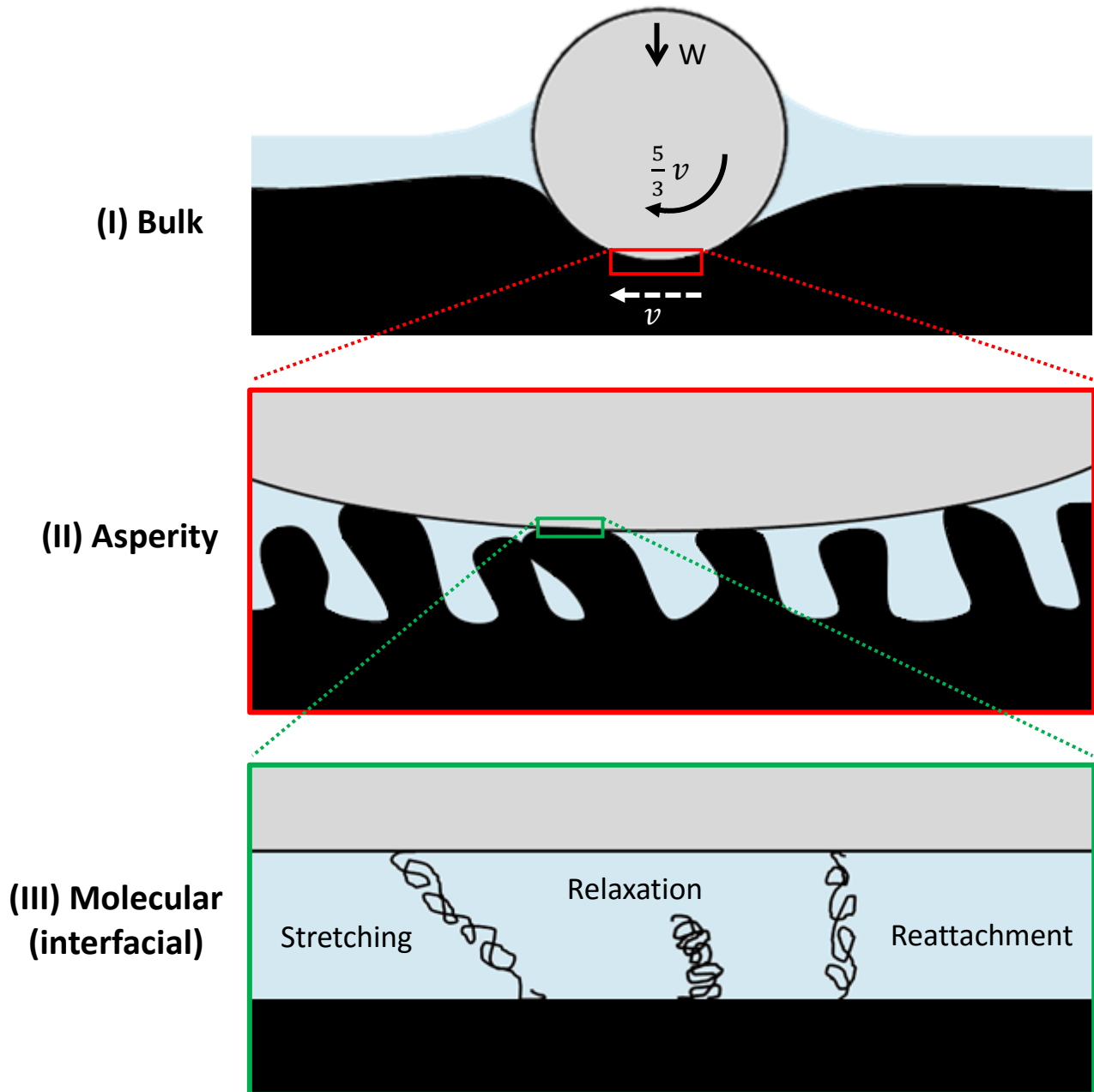
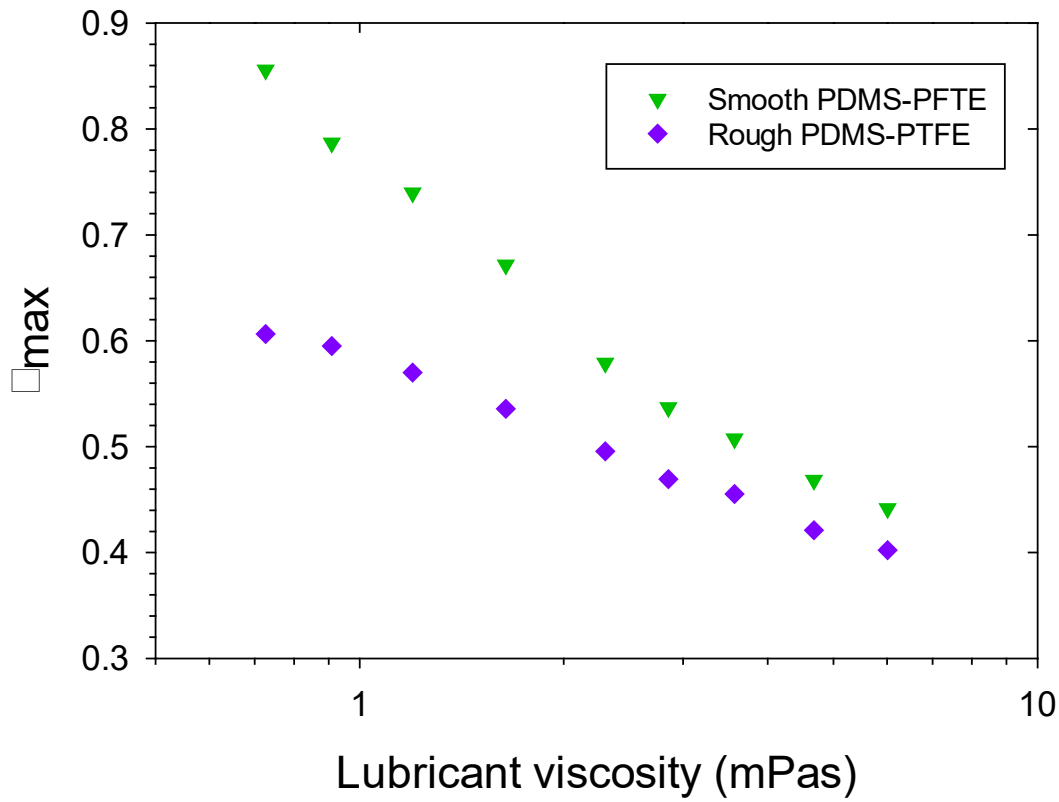
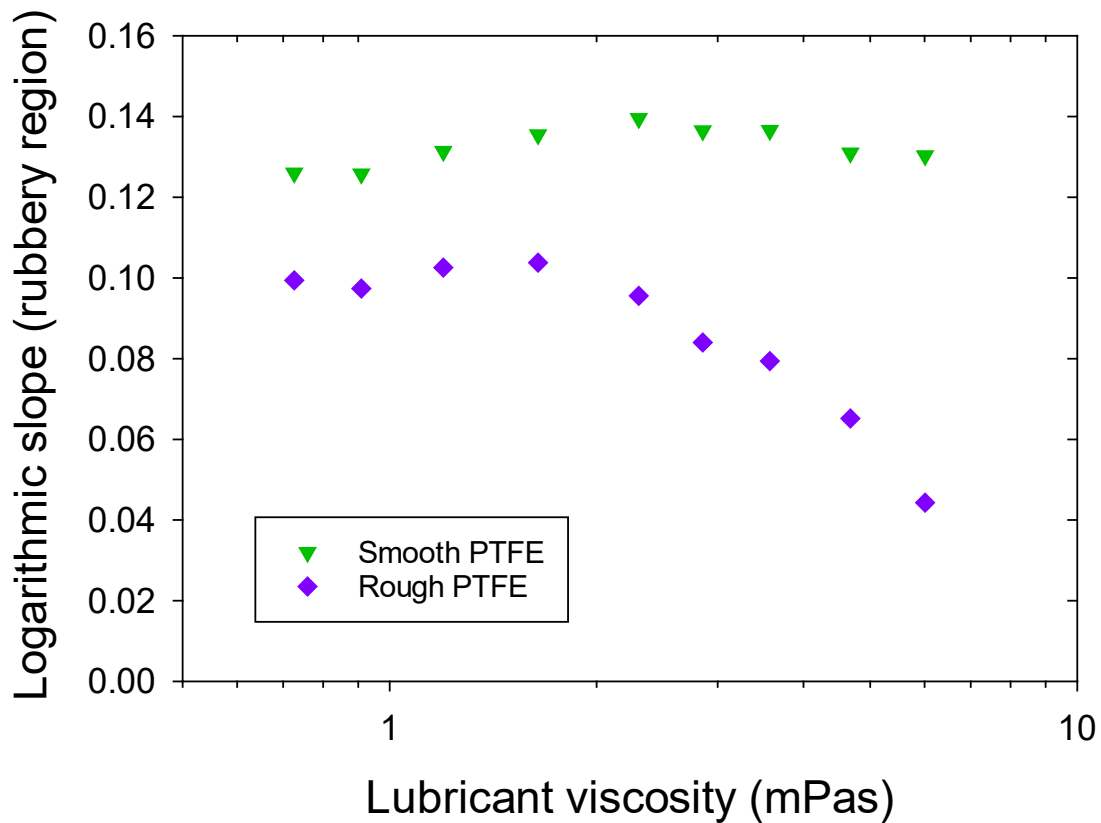
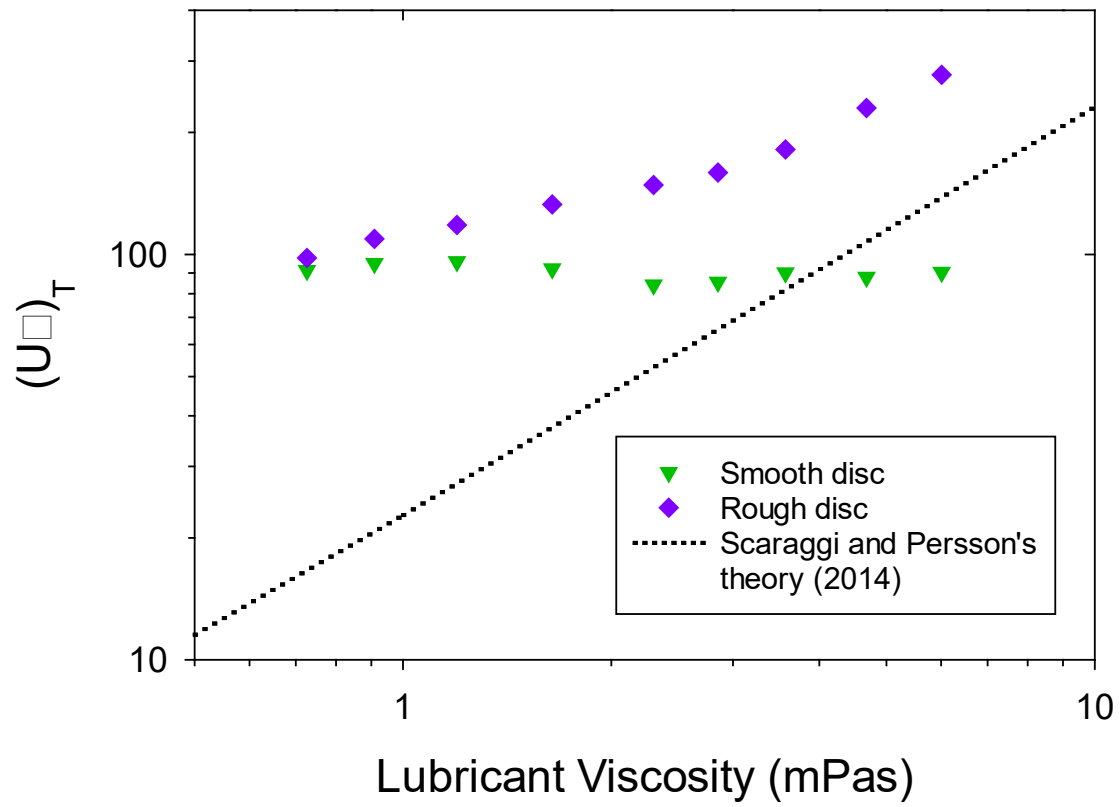


Figure 5**A****B**

C



Supplementary Information

(I) Calculation of Hertzian contact parameters:

The contact radius is given by:

$$a = \sqrt[3]{3WR/4E'}$$

where W is the load, R is the PTFE ball radius and E' is defined by the following equation:

$$\frac{2}{E'} = \frac{1 - \nu_1^2}{E_1} + \frac{1 - \nu_2^2}{E_2}$$

The indentation depth is given by:

$$\delta = \frac{a^2}{R}$$

For the PTFE ball-PDMS disc contact used in this tribological study, the values of the variables are as follows:

$$W = 2 \text{ N}$$

$$R = 9.25 \text{ mm}$$

$$E_1 = 0.5 \text{ GPa (PTFE)}$$

$$E_2 = 2.4 \text{ MPa (PDMS)}$$

$$\nu_1 = 0.5 \text{ (PTFE)}$$

$$\nu_2 = 0.46 \text{ (PDMS)}$$

This yields a contact radius of 1.30 mm and an indentation depth of 181.7 μm .